HHS Public Access

Author manuscript

Am J Surg Pathol. Author manuscript; available in PMC 2021 March 01.

Published in final edited form as:

Am J Surg Pathol. 2020 March ; 44(3): 368–377. doi:10.1097/PAS.0000000000001382.

Recurrent *YAP1* and *KMT2A* Gene Rearrangements in a Subset of MUC4-Negative Sclerosing Epithelioid Fibrosarcoma

Yu-Chien Kao, MD[#1,*], **Jen-Chieh Lee, MD, PhD**[#2,*], **Lei Zhang, MD**[3], **Yun-Shao Sung, MSc**[3], **David Swanson, BSc**[4], **Tsung-Han Hsieh, PhD**[5], **Yun-Ru Liu, PhD**[5], **Narasimhan P Agaram, MD**[3], **Hsuan-Ying Huang, MD**[6], **Brendan C. Dickson, MD**[4], **Cristina R. Antonescu, MD.**[3]

[1]Department of Pathology, Shuang Ho Hospital, Taipei Medical University, Taipei, Taiwan

[2]Department and Graduate Institute of Pathology, National Taiwan University Hospital, National Taiwan University College of Medicine, Taipei, Taiwan

[3]Department of Pathology, Memorial Sloan Kettering Cancer Center, New York, NY, USA

[4]Department of Pathology & Laboratory Medicine, Mount Sinai Hospital, Toronto, Canada

[5]Joint Biobank, Office of Human Research, Taipei Medical University, Taipei, Taiwan

[6]Department of Anatomical Pathology, Kaohsiung Chang Gung Memorial Hospital and Chang Gung University College of Medicine, Kaohsiung, Taiwan

[#] These authors contributed equally to this work.

Abstract

Sclerosing epithelioid fibrosarcoma (SEF) is an aggressive soft tissue sarcoma, characterized by a distinctive epithelioid phenotype in a densely sclerotic collagenous stroma, that shows frequent MUC4 immunoreactivity and recurrent gene fusions, often involving *EWSR1* gene. A pathogenetic link with low grade fibromyxoid sarcoma (LGFMS) has been suggested, due to cases with hybrid morphology as well as overlapping genetic signature. However, a small subset of SEF is negative for MUC4 and lacks the canonical *EWSR1*/*FUS* gene rearrangements. Triggered by the identification of recurrent *YAP1-KMT2A* gene fusions by RNA sequencing in 3 index cases of MUC4-negative, *EWSR1*/*FUS* fusion-negative SEF, we further investigated a cohort of 14 similar SEF cases (MUC4-negative, *EWSR1*/*FUS* fusion-negative) by fluorescence in situ hybridization (FISH), reverse transcription polymerase chain reaction (RT-PCR), and/or DNA-based massively parallel sequencing (MSK-IMPACT) for abnormalities in these genes. Three additional SEFs with *KMT2A* gene rearrangements and one additional case with *YAP1* gene rearrangements were identified by FISH. In addition, one case with *YAP1-KMT2A* and one with *KMT2A-YAP1* fusion were detected by RT-PCR and MSK-IMPACT, respectively. As a control group, 24 fibromyxoid spindle cell tumors, diagnosed or suspected as fusion-negative LGFMS, were also tested for *YAP1* and *KMT2A* abnormalities by FISH, but none were positive. The *YAP1*/*KMT2A*-rearranged SEF group affected patients ranging from 10–73 years old (average & median: 45) of both genders (4 females, 5 males). The tumors involved somatic soft tissues with a wide distribution, including

Correspondence: Cristina R. Antonescu, MD, Memorial Sloan Kettering Cancer Center, 1275 York Ave, New York, NY 10065. antonesc@mskcc.org.

[*]These authors contributed equally.

extremities, trunk, pelvis, neck, and dura. Histologically, the tumors showed variable cellularity, with monotonous ovoid to epithelioid tumor cells and hyalinized collagenous background typical of SEF. More than half of the cases showed infiltrative borders, within fat or skeletal muscle. No LGFMS component was identified. All tumors were negative for MUC4 and had an otherwise non-specific immunophenotype. Of the 6 cases with available follow-up information, 2 had local recurrences, and 2 developed soft tissue and/or bone metastases, including 1 of them died of the disease.

Keywords

Sclerosing epithelioid fibrosarcoma; Low-grade fibromyxoid sarcoma; *YAP1*; *KMT2A*; *MLL*; MUC4

INTRODUCTION

Sclerosing epithelioid fibrosarcoma (SEF) is a highly aggressive soft tissue sarcoma closely related to low-grade fibromyxoid sarcoma (LGFMS).[1,2] Some tumors display morphologic characteristics of both SEF and LGFMS, being classified as hybrid SEF/LGFMS. Furthermore, SEF and LGFMS share overexpression of MUC4 by immunohistochemistry. Although MUC4 immunohistochemistry represents a sensitive and specific marker for LGFMS,[3] it is only present in up to 78% of SEFs.[4] At the genetic level, a molecular dichotomy between these two tumors has emerged, with pure SEF harboring mostly *EWSR1-CREB3L1* fusions, while LGFMS and hybrid SEF/LGFMS displaying *FUS-CREB3L2* fusions.[5,6] Nevertheless, significant morphologic, immunohistochemical and cytogenetic overlap exists in a minority of cases.

Triggered by a handful of cases with the morphologic appearance of SEF, but lacking MUC4 expression and the typical *EWSR1/FUS* gene rearrangements, we have explored their molecular abnormalities using a combined approach using targeted RNA sequencing, targeted DNA sequencing, fluorescence in situ hybridization (FISH), and/or reverse transcription polymerase chain reaction (RT-PCR) methodology. The recurrent genetic alterations identified were then screened in a larger cohort of cases.

MATERIALS AND METHODS

Index cases and cohort selection screening

Three index cases of soft tissue tumors with a histomorphology resembling SEF, but lacking MUC4 immunoreactivity and *EWSR1*/*FUS* gene rearrangements, were submitted to targeted RNA sequencing for fusion discovery. These patients were all in their forties, with tumors involving somatic soft tissues, including two in the lower extremities (thigh, lower leg) and one in the trunk (paraspinal) (Table 1). After identification of the fusion candidates, fluorescence in situ hybridization (FISH) was performed on all 3 cases, using a custom break-apart probe design of the respective fusion partner genes, in order to validate the gene rearrangements. Reverse transcription polymerase chain reaction (RT-PCR) was performed on case #3, using primers designed based on the fusion junction reads of RNA sequencing.

To further investigate the prevalence of the identified gene fusions in SEF and the closely related low-grade fibromyxoid sarcoma (LGFMS) and to better understand the clinicopathologic spectrum of such tumors, the consultation archive of the senior author (C.R.A.) was searched for cases diagnosed as or suspected to be SEF and LGFMS, which were negative for MUC4 immunostain and *EWSR1*/*FUS* gene rearrangements. The resultant screening cohorts of SEF (n=14) and LGFMS (n=24) were studied using break-apart FISH assays for *YAP1* and *KMT2A* rearrangements. Cases with available material were also tested by RT-PCR for *YAP1-KMT2A* fusion. As part of the clinical work-up for diagnostic and therapeutic purposes, one SEF case was subjected to MSK-IMPACT (Memorial Sloan Kettering Cancer Center Integrated Mutation Profiling of Actionable Cancer Targets), a targeted DNA-based next generation sequencing using hybridization capture strategy as described previously.

Clinical follow-up information was obtained from the electronic medical records or the initial referral pathologists. The study was approved by the Institutional Review Board.

RNA sequencing and data analysis

Cases #1 and #2 were submitted to targeted RNA sequencing using TruSight RNA Fusion Panel (Illumina, San Diego, CA), while case #3 was studied using TruSeq RNA Exome (Illumina, San Diego, CA). RNA was extracted from formalin-fixed paraffin-embedded (FFPE) tissues, using Amsbio's ExpressArt FFPE Clear RNA Ready kit (Amsbio LLC, Cambridge, MA) in cases #1 and #2, or RNeasy FFPE kit (Qiagen, USA) in case#3, according to the manufacturer's instructions. Fragment length was assessed with an Agilent Bioanalyzer (Agilent Technologies, Santa Clara, CA). For cases #1–2, RNA sequencing libraries were prepared using 20–100 ng total RNA with the Trusight RNA Fusion Panel. Each sample was subjected to targeted RNA sequencing on an Illumina MiSeq at 8 samples per flow cell (approximately 3 million reads per sample). Sample#3 was ligated to adaptors for further amplification and exonic region enrichment using TruSeq RNA Exome, which focuses on capturing the coding regions of RNA. All reads were independently aligned with STAR (ver 2.3) and BowTie2 against the human reference genome (hg19) for Manta-Fusion or STAR-Fusion and TopHat-Fusion analysis, respectively.

Reverse transcription polymerase chain reaction (RT-PCR)

RT-PCR was performed on case #3 to validate the gene fusion and on one case (case #8) from the screening cohort. The primer sequences were designed based on the fusion junction read sequences from RNA sequencing (Supplementary Table 1). RNA after RNA sequencing was subjected to reverse transcription using SuperScript IV First-Strand Synthesis System (Invitrogen). PCR was performed by Phusion Green Hot Start II High-Fidelity DNA Polymerase (Thermo Scientific). The PCR products were then analyzed by gel electrophoresis and Sanger sequencing.

Fluorescence in situ hybridization (FISH)

FISH was performed on 4 μm-thick FFPE tissue sections. Custom probes were made by bacterial artificial chromosomes (BAC) clones (Supplementary Table 2) flanking *YAP1, KMT2A,* and *MAML2,* and flanking/covering *VIM* genes, according to UCSC genome

browser (http://genome.ucsc.edu) and obtained from BACPAC sources of Children's Hospital of Oakland Research Institute (Oakland, CA; https://bacpacresources.org). Fusion FISH assays were also performed on selected cases. DNA from each BAC was isolated according to the manufacturer's instructions. The BAC clones were labeled with fluorochromes by nick translation and validated on normal metaphase chromosomes. The slides were deparaffinized, pretreated, and hybridized with denatured probes. After overnight incubation, the slides were washed, stained with DAPI, mounted with an antifade solution, and then examined on a Zeiss fluorescence microscope (Zeiss Axioplan, Oberkochen, Germany) controlled by Isis 5 software (Metasystems, Newton, MA).

RESULTS

A recurrent *YAP1-KMT2A* fusion is identified in MUC4-negative SEFs

A *YAP1-KMT2A* fusion candidate was identified in all 3 index cases tested by 2 different RNA sequencing platforms. The fusions joined *YAP1* exon 5 (NM_001130145) to *KMT2A* exon 4 (NM_001197104) in cases #1 and #3, and *YAP1* exon 4 to *KMT2A* exon 5 in case #2 (Fig. 1). Both fusion transcript variants were predicted to be in-frame. In case #3, a variant *YAP1-KMT2A* fusion transcript was noted by RNA sequencing, showing an additional 12 bp of *YAP1* intron 5 at the fusion juction, possibly due to alternative splicing. In addition, the reciprocal *KMT2A-YAP1* fusion transcripts were present in all 3 cases, as *KMT2A* exon 6-*YAP1* exon 9 (in-frame) in cases #1 and #3 and *KMT2A* exon 5-*YAP1* exon 9 (breakpoints within exons, out-of-frame) in cases #2. RT-PCR confirmed the *YAP1-KMT2A* and *KMT2A-YAP1* fusions in case #3 (Fig. 2A).

In the screening cohort, one case (case #8) with available material was subjected to RT-PCR using the same primers and was shown to have the same *YAP1* exon 5-*KMT2A* exon 4 fusion. No reciprocal *KMT2A* exon 6 - *YAP1* exon 9 fusion transcript was found by RT-PCR. The case (case #9) studied by MSK-IMPACT showed fusion of *KMT2A* intron 6–7 (100bp) to *YAP1* intron 8–9 (339bp). The predicted *KMT2A* exon 6-*YAP1* exon 9 fusion transcript was identical to the reciprocal fusion transcripts found in cases #1 and #3 by RNA sequencing.

YAP1 and *KMT2A* rearrangements appear cryptic, not commonly detectable at the FISH resolution

FISH for *YAP1* and *KMT2A* abnormalities were performed on the above-mentioned 5 cases with known *YAP1* and *KMT2A* fusion sequences (cases #1–3, 8, 9). The presence of an *YAP1* break-apart was observed only in case #3 (Fig. 2B), which showed one fused normal signal and one abnormal signal (single green, telomeric probe). In other cases, no *YAP1* break-apart was detected by FISH, though cases #1, 2 and 9 had only 1 normal copy of *YAP1*. FISH for *KMT2A* rearrangements were negative in all 5 cases. Fusion FISH assay using telomeric probe of *YAP1* (green) and centromeric probe of *KMT2A* was performed on case #3, but was negative for gene fusion. These findings suggest that *YAP1* and *KMT2A* gene rearrangements in these tumors are often cryptic and beyond the FISH resolution. *YAP1* and *KMT2A* genes are both located on chromosome 11q with the same direction of transcription, with a 16 Mb distance between these 2 genes. Based on the results of case# 3,

it is likely that only a small fragment of the *YAP1* locus is retained in the fusion event, being associated with a large deletion of the nearby locus (as demonstrated by the loss of the red, centromeric probe). Therefore, FISH studies may not represent the appropriate tool for screening, being associated with a high false-negative rate in these tumors.

Alternative fusion partners may occur in *YAP1* or *KMT2A*-rearranged SEF

Four additional cases with either *YAP1* or *KMT2A* gene abnormalities were identified by FISH in the remaining SEF screening cohort, 1 with *YAP1* rearrangement and 3 with *KMT2A* rearrangements (Fig. 2C, Table 1). None of them showed concurrent *YAP1* and *KMT2A* rearrangements by FISH. Fusion FISH assays of *YAP1-KMT2A* also showed negative results (cases #5–7). Case #4 showed a *KMT2A* gene rearrangement and only one normal copy of *YAP1*. To investigate other potential fusion gene partners, FISH for *VIM* and *MAML2* gene rearrangements, two recently described fusion partners of *YAP1* or *KMT2A* gene[7–14], were performed on cases #4–7. Case #5 (*KMT2A*-rearranged) showed an additional *MAML2* break-apart; a gene also located in chromosome 11q. Although FISH fusion assay using probes flanking *MAML2* and centromeric to *KMT2A* did not show a fused signal between *MAML2* and *KMT2A,* the possibility of a *KMT2A-MAML2* fusion cannot be excluded considering the complex abnormalities and high false negative rates of FISH method in the index cases. Cases #4, 6 and 7 were negative for *MAML2* rearrangements, and all 4 cases tested lacked abnormalities in *VIM* gene by FISH.

YAP1 and/or *KMT2A*-rearranged SEFs show infiltrative borders and a deceptively hypocellular morphology

In total, 9 cases, including the 3 index cases and 6 additional from the screening cohort, were identified as harboring rearrangements in *YAP1* and/or *KMT2A* genes (Table 1). The patients ranged from 10–73 years old (average & median: 45), with 6 (67%) patients diagnosed above the age of 40 years, in both genders (5 male and 4 female patients). The tumors involved mainly somatic soft tissues of the trunk and lower extremities, either superficial or deep-seated, including thigh, lower leg, inguinal area, iliopsoas muscle, paraspinal, and chest wall. Two tumors affected the head and neck region. One of them (case #6) presented as a brain tumor and involved frontal lobe dura, with secondary bone erosion, in a 10-year-old girl. The other was a large, unresectable cervical neck/paraspinal soft tissue mass of a 22-year-old (case #9) involving the brachial plexus. Tumor sizes ranged from 2.0 to 12.0 cm.

The morphology of the primary tumors was reviewed in all except 2 cases (#2 and #3), for which material was only available from the metastatic tumor and 3 recurrent tumors, respectively. Histologically, at least half of the cases showed infiltrative borders (5/9; 56%). Three tumors entrapped adipocytes from adjacent subcutaneous tissue (cases #4, 5 and 8) (Fig. 3A). Skeletal muscle infiltration was seen in case #1 and in the second recurrence of case #3 (Fig. 3B). Most tumors showed zonal variation in cellularity, ranging from low, intermediate, to high (Fig. 3C). The more cellular areas were often observed at the periphery (n=4), but occasionally were also noted intermixed with less cellular areas in the tumor (n=2) or as scattered small cellular foci in the center (n=1). The tumor cells ranged from rounded, ovoid, to epithelioid, with monotonous nuclei, fine chromatin, and small nucleoli

(Fig. 3D–F). Short spindle cells arranged in a storiform growth were also seen in some cases as a focal pattern (Fig. 4A). Case #6 in addition showed more elongated spindle cells arranged in fascicles (Fig. 4B). Mitotic activity ranged widely, from 0 to 21 per 10 high power fields. The background stroma was hyalinized and sclerotic in all cases, including homogeneous fibrous background, thick collagenous bundles, and delicate dense collagen fibers enveloping individual tumor cells resembling osteoid matrix (Fig. 4C–E). Thin-walled dilated vessels were present in the tumor in about half of the cases (Fig. 3F, 4F). Intravascular tumor protrusion was seen in one case. Deceptively hypocellular fibroma-like areas composed of bland small ovoid cells in densely collagenous stroma were present in 5 cases and led to the initial diagnoses of benign lesions, including fibrous lesion, benign fibrous histiocytoma, and desmoid tumor (cases #1–3) (Fig. 4C, 4F). None of them showed areas of LGFMS morphology, lacking the typical alternating fibrous and myxoid components, with delicate spindle cells arranged in a swirling pattern. Recurrent tumors showed increased cellularity (case #1, third recurrence of case #3) (Fig. 4A), and osseous metaplasia was observed in the 3rd recurrence of case #3 (21 years after initial diagnosis).

All tumors were negative for MUC4 immunostaining. Other immunostains were negative or non-specific. S100 stain showed patchy staining in about half of the cases tested (3/7), but they were negative for SOX10 in 5 cases tested. Multifocal weak EMA, focal CD34, ERG, and focal desmin expressions were seen in the 5/7, 3/7, 1/3, and 1/7 cases tested, respectively. Variable intensity of BCOR (4/4; weak in 2, moderate in 1, strong in 1) and strong cyclin D1 (2/2) staining were also seen. CD31 (n=3), beta-catenin (n=3), and SMA (n=5) stains were negative.

Of the 6 cases with available follow-up information, local recurrence and distant metastasis were observed in 2 patients each. Case #1 underwent a piecemeal excision of the paraspinal tumor and had local recurrence 1 year later. The recurrent tumor was treated with neoadjuvant radiotherapy and resection. The recurrent specimen showed increased cellularity compared to the primary tumor. No further follow-up was available after the resection. Case #2 had a subcutaneous thigh mass which was excised with free margins and developed soft tissue metastasis 1.5 years later. Case #3 presented as a 2.0 cm intramuscular tumor of the lower leg which was treated with surgery alone and subsequently developed multiple late recurrences 10, 17, and 21 years after the diagnosis. No metastasis was observed. Case #4, a deep-seated tumor involving the iliopsoas muscle and adjacent bone in a 73-year-old, developed bone and soft tissue metastases to the contralateral pelvis and scalp and died of the disease 1 year after diagnosis. Case #6, a dural-based tumor of a 10-year-old, showed no evidence of disease 2.5 years after the surgery. Lastly, case#9 was unresectable and the patient received chemotherapy with some decrease in tumor size, and is alive with disease 1 year later.

MUC4-negative low-grade fibromyxoid sarcomas lacked *YAP1* or *KMT2A* gene alterations

Considering the overlapping clinicopathologic and genetic characters of SEF and LGFMS, a screening cohort of 24 MUC4-negative fibromyxoid spindle cell tumors, diagnosed or suspected as fusion-negative LGFMS, were also examined by FISH for *YAP1* and *KMT2A* abnormalities. All these cases showed no evidence of *YAP1* and *KMT2A* gene

rearrangements. However, due to high false negative rate by FISH in detecting this fusion, further studies using other methodologies are needed to clarify if this genetic group is truly only observed in SEF but not in LGFMS cases, unlike the *EWSR1*/*FUS* gene rearrangements.

DISCUSSION

Sclerosing epithelioid fibrosarcoma is a rare soft tissue tumor exhibiting a characteristic morphologic pattern of epithelioid cells arranged in strands, cords, nests and sheets embedded in a sclerosed and hyalinized stroma.[1,2] A subset of SEF shares morphologic overlap with low grade fibromyxoid sarcoma, that features a deceptively benign histology of bland appearing spindle cells in an alternating fibrous and myxoid stroma.[15,16]. SEF tends to have an aggressive clinical course with high rates of local recurrence (50%), distant metastasis (40–80%) and mortality (25–57%).[1,2] Although LGFMS have been initially described as following a protracted clinical course with local recurrences and late metastasis, [15,16] in a more recent comprehensive study of 33 LGFMS cases with long-term follow-up (mean of 14 years), half of the patients developed metastases and 42% died of disease.[17]

MUC4 was found to be among the top upregulated genes in LGFMS and thus detectable at the protein level;[18] with subsequent comprehensive studies demonstrating that MUC4 immunohistochemistry represents a sensitive and specific marker for this entity.[3] Expression of MUC4 was also demonstrated in the majority but not all SEF cases (up to 78%),[4] suggesting a certain heterogeneity in this group of tumors. Moreover, in our prior study, only one *EWSR1*-rearranged pure SEF was negative for MUC4 staining, while all the SEF/LGFMS hybrid tumors tested expressed MUC4.[6] Additionally, a *FUS-CREB3L2* translocation positive, MUC4-negative LGFMS was also recently published.[19]

At the genetic level, most pure SEF cases showed *EWSR1-CREB3L1* fusions, while the overwhelming majority of hybrid SEF/LGFMS lesions are characterized by *FUS-CREB3L2*.[5,6] With few exceptions,[6,19] *EWSR1* and *FUS*-rearranged SEF cases are often MUC4 positive,[4,6] while the molecular pathogenesis of MUC4-negative SEF remains unknown. In this study, we demonstrated that at least half (9/17, including index cases and screening cohort) of MUC4-negative SEF harbors *YAP1* and/or *KMT2A* gene rearrangements.

YAP1-KMT2A fusions have been reported in rare sarcoma cases.[7,20] A chest wall tumor diagnosed as ‘sclerosing fibrosarcoma’ in a 35-year-old female was found to have *YAP1-KMT2A* fusion by RNA sequencing in a large-scale study focused on small round cell sarcomas.[20] Although the histomorphology and immunoprofile of this case are not available, it is likely that it also falls into the morphologic spectrum of SEF as our cases. More recently, two sarcoma cases with *KMT2A* rearrangements, fused with *YAP1* and *VIM*, respectively, were identified by RNA sequencing.[7] The first case harboring a *YAP1-KMT2A* fusion presented in a 20-year-old female with a deep thigh tumor (8.5 cm) showing similar histomorphology to our cases, with infiltrative borders, epithelioid to round cells embedded in a sclerotic stroma, and focal storiform growth of short spindle cells. Immunohistochemically, this case showed focal EMA, CD31, CD34, and ERG staining, and

was negative for MUC4. Some of these markers were also focally positive in some of our cases, however none of our cases showed CD31 positivity (tested in 3 cases). Similar to our cases (#1, 3, and 8), the exon composition of their case included a *YAP1* exon 5- *KMT2A* exon 4 fusion transcript. Although the reciprocal *KMT2A-YAP1* fusion transcript was present in the majority of these tumors reported to date and the number of reciprocal fusion reads exceeded *YAP1-KMT2A* reads in some of our cases, the immunoreactivity to the N-terminal YAP1 but not C-terminal YAP1 is in keeping with a *YAP1-KMT2A* being the main functional transcript.[7]

Their second case, harboring a *VIM-KMT2A* fusion, presented in a 30 year-old woman with a femoral bone lesion,[7] displayed a somewhat distinct morphology from our cases. It showed a hypercellular round to spindle cell morphology, with a sclerotic stroma being more prominent in the resection specimen after chemotherapy. We examined our *KMT2A* rearranged cases with unknown fusion partners for *VIM* gene abnormalities by FISH, but did not identify any positive cases. In addition to focal EMA positivity, the *VIM-KMT2A* case also showed immunoreactivity to BCOR (diffuse strong), WT1, and NKX2.2. BCOR staining was also observed in all 4 cases tested in our study, but more commonly with a non-specific weak to moderate intensity. By RNA sequencing data, our cases #1–3 did not show significant up-regulation of *WT1* and *NKX2.2*. Both of their patients developed pulmonary and/or bone metastases and died of disease.[7]

The present study expands the clinicopathologic spectrum of sarcomas harboring *YAP1-KMT2A* fusions. Our patients ranged from 10 to 86 years old. In addition to chest wall and lower extremities, some cases involved the paraspinal soft tissue, neck, and dura. Some of our patients presented with large and deep-seated tumors, like most SEF with *EWSR1*/*FUS* fusions and the previously reported *YAP1-KMT2A* positive sarcomas; while others were smaller in size and involved superficial subcutaneous tissues only. Our results also showed a more variable clinical course, with some patients developing early metastases and others having prolonged multiple recurrence or being disease free. Further larger studies are needed to better determine their biologic potential and prognostic significance of different fusion genotypes in SEF.

Our study also pointed out that this intra-chromosomal 11 translocation resulting in a *YAP1-KMT2A* fusion is likely complex and unbalanced, rather than a simple translocation or interstitial deletion, as it is often not detected by either break-apart or fusion FISH assays. *YAP1* (11q22.1–22.2) and *KMT2A* (11q23.3) are both located on the long arm of chromosome 11, 16 Mb apart, with the same direction of transcription. These findings may explain the high false-negative rate of the FISH assays, as none of our 3 index cases with *YAP1-KMT2A* fusions by RNA sequencing revealed *KMT2A* rearrangements and only one case showed *YAP1* split signals. Therefore, the prevalence of this fusion among MUC4-negative SEF is expected to be higher.

Awareness of the existence of MUC4-negative SEF and its potential aggressive behavior is crucial. Some of the tumors in our cohort showed deceptively bland hypocellular fibrous morphology, similar to the previously described fibroma-like area in SEF,[2] and only focally the more cellular areas with round to epithelioid tumor cells in a sclerotic stroma, and

therefore could be misdiagnosed as benign tumors or tumors with intermediate behavior, such as fibrous histiocytoma, desmoid tumor, solitary fibrous tumor, etc. In addition, although hypocellular areas were observed in 5 of 9 cases, none of them showed fibromyxoid stroma typical of LGFMS.

KMT2A (*MLL*), a transcriptional coactivator with H3K4 methyltransferase activity, is a well-known gene involved in genetic rearrangements in leukemias, including infantile, pediatric, adult and therapy-induced leukemias, and are associated with poor outcome.[21] In *KMT2A*-rearranged leukemia, *KMT2A* is the 5' fusion partner gene and most commonly fused to *AF4*, *AF9*, *AF10*, and *ENL*, among many other fusion partners. The most prevalent breakpoints of *KMT2A* in *KMT2A*-rearranged leukemia are between exon 9 and intron 11, resulting in retained N-terminal DNA binding domains but losing the C-terminal SET domain with H3K4 methyltransferase activity in the chimeric protein.[21] In SEF cases, *KMT2A* is presumably the 3' fusion partner gene and the most common breakpoints were observed in exons 4–5, resulting in a partially disrupted or totally lost DNA binding domain and intact SET domain. In our index cases, RNA sequencing showed no significant up-regulation of *YAP1* or *KMT2A*, while the *KMT2A* expression levels were even slightly lower than control (data not shown). We also did not observe up-regulation of the target genes of *KMT2A,* such as *HOXA9* and *MEIS*, which are up-regulated in *KMT2A*-rearranged leukemia.[22] Nevertheless, in the previously reported sarcoma with *VIM-KMT2A* fusion, up-regulation of *KMT2A* and *HOXA* genes were noted.[7] The pathogenic mechanism of *KMT2A*-rearranged sarcoma remains to be explored.

One of our cases (case #5) showed rearrangements of both *KMT2A* and *MAML2* genes by FISH. *MAML2* (11q21) is also located on chromosome 11, centromeric to *YAP1* and *KMT2A* and in the opposite transcriptional direction. It has been reported as rare fusion partners of *KMT2A* in leukemias.[8–10] Since 3 of our cases had only *KMT2A* or *YAP1* rearrangements by FISH, other alternative fusion partner genes likely exist.

Our case #6 stood out in this study cohort with regard to the particularly young age of 10 years, the unusual dura location, and the round to elongated spindle cell morphology. Areas more typical of SEF with dense sclerotic collagen fibers enveloping ovoid to rounded tumor cells were present and alternating with the fascicular spindle cell areas. Interestingly, a dura-based spindle cell tumor with *MN1-KMT2A* fusion has been reported recently in a 22-year-old female.[23] However, the morphology of that case is composed of more plump spindle cells arranged in hypercellular sheets and fascicles, lacking the sclerotic stroma as identified in our case, and expresses diffuse and strong S-100 and PR staining. FISH for *MN1* gene rearrangement was negative in our case #6, as was S100 protein staining.

YAP1, a downstream effector of the Hippo signaling pathway, is also known to be involved in recurrent gene fusions in a subset of epithelioid hemangioendothelioma (*YAP1-TFE3*) and ependymoma (*YAP1- MAMLD1* and *FAM118B*).[24,25] In *YAP1-KMT2A* fusions, the N-terminal TEAD binding domain of *YAP1* is retained, while the C-terminal transcriptional activation domain is lost. Interestingly, *YAP1-MAML2* fusions through chromosomal inversions have also been described in poroma (88.5%), porocarcinoma (63.6%), and rare

cases of various carcinoma types.[11–14] Our case #7 also showed an inversion pattern of *YAP1* rearrangement by FISH, but was negative for *MAML2* rearrangements by FISH.

In summary, we report a group of MUC4-negative SEF with *YAP1* and/or *KMT2A* gene rearrangements. While many of the clinicopathologic features overlap with MUC4-positive SEF, these tumors in particular can present as superficial and small tumors with infiltrative borders and could be deceptively fibrotic and hypocellular, mimicking benign lesions. Due to the lack of specific immunohistochemical markers at this point and the high false negative rate by FISH, a high index of suspicion and incorporating different diagnostic methodology, including next generation sequencing, are needed to avoid misdiagnosis.

Supplementary Material

Refer to Web version on PubMed Central for supplementary material.

ACKNOWLEDGMENTS

The authors thank Dr. Chung-Hsi Wang, Dr. Cheng-Hsiang Hsiao, and Dr. Chin-Cheng Lee for contribution of cases and providing the follow-up information.

Disclosures: Supported in part by: P50 CA 140146-01 (CRA), P50 CA217694 (CRA), P30 CA008748, Cycle for Survival (CRA), Kristin Ann Carr Foundation (CRA), St Baldrick Foundation (CRA)

REFERENCES

1. Meis-Kindblom JM, Kindblom LG, Enzinger FM. Sclerosing epithelioid fibrosarcoma. A variant of fibrosarcoma simulating carcinoma. Am J Surg Pathol. 1995;19:979–993. [PubMed: 7661286]
2. Antonescu CR, Rosenblum MK, Pereira P, et al. Sclerosing epithelioid fibrosarcoma: a study of 16 cases and confirmation of a clinicopathologically distinct tumor. Am J Surg Pathol. 2001;25:699–709. [PubMed: 11395547]
3. Doyle LA, Moller E, Dal Cin P, et al. MUC4 is a highly sensitive and specific marker for low-grade fibromyxoid sarcoma. Am J Surg Pathol. 2011;35:733–741. [PubMed: 21415703]
4. Doyle LA, Wang WL, Dal Cin P, et al. MUC4 is a sensitive and extremely useful marker for sclerosing epithelioid fibrosarcoma: association with FUS gene rearrangement. Am J Surg Pathol. 2012;36:1444–1451. [PubMed: 22982887]
5. Arbajian E, Puls F, Magnusson L, et al. Recurrent EWSR1-CREB3L1 gene fusions in sclerosing epithelioid fibrosarcoma. Am J Surg Pathol. 2014;38:801–808. [PubMed: 24441665]
6. Prieto-Granada C, Zhang L, Chen HW, et al. A genetic dichotomy between pure sclerosing epithelioid fibrosarcoma (SEF) and hybrid SEF/low-grade fibromyxoid sarcoma: a pathologic and molecular study of 18 cases. Genes Chromosomes Cancer. 2015;54:28–38. [PubMed: 25231134]
7. Yoshida A, Arai Y, Tanzawa Y, et al. KMT2A (MLL) fusions in aggressive sarcomas in young adults. Histopathology. 2019.
8. Menu E, Beaufils N, Usseglio F, et al. First case of B ALL with KMT2A-MAML2 rearrangement: a case report. BMC Cancer. 2017;17:363. [PubMed: 28535805]
9. Metzler M, Staege MS, Harder L, et al. Inv(11)(q21q23) fuses MLL to the Notch co-activator mastermind-like 2 in secondary T-cell acute lymphoblastic leukemia. Leukemia. 2008;22:1807–1811. [PubMed: 18337764]
10. Nemoto N, Suzukawa K, Shimizu S, et al. Identification of a novel fusion gene MLL-MAML2 in secondary acute myelogenous leukemia and myelodysplastic syndrome with inv(11)(q21q23). Genes Chromosomes Cancer. 2007;46:813–819. [PubMed: 17551948]
11. Sekine S, Kiyono T, Ryo E, et al. Recurrent YAP1-MAML2 and YAP1-NUTM1 fusions in poroma and porocarcinoma. J Clin Invest. 2019;130.

12. Valouev A, Weng Z, Sweeney RT, et al. Discovery of recurrent structural variants in nasopharyngeal carcinoma. Genome Res. 2014;24:300–309. [PubMed: 24214394]
13. Papp E, Hallberg D, Konecny GE, et al. Integrated Genomic, Epigenomic, and Expression Analyses of Ovarian Cancer Cell Lines. Cell Rep. 2018;25:2617–2633. [PubMed: 30485824]
14. Picco G, Chen ED, Alonso LG, et al. Functional linkage of gene fusions to cancer cell fitness assessed by pharmacological and CRISPR-Cas9 screening. Nat Commun. 2019;10:2198. [PubMed: 31097696]
15. Evans HL. Low-grade fibromyxoid sarcoma. A report of two metastasizing neoplasms having a deceptively benign appearance. Am J Clin Pathol. 1987;88:615–619. [PubMed: 3673943]
16. Evans HL. Low-grade fibromyxoid sarcoma. A report of 12 cases. Am J Surg Pathol. 1993;17:595–600. [PubMed: 8333558]
17. Evans HL. Low-grade fibromyxoid sarcoma: a clinicopathologic study of 33 cases with long-term follow-up. Am J Surg Pathol. 2011;35:1450–1462. [PubMed: 21921785]
18. Moller E, Hornick JL, Magnusson L, et al. FUS-CREB3L2/L1-positive sarcomas show a specific gene expression profile with upregulation of CD24 and FOXL1. Clin Cancer Res. 2011;17:2646–2656. [PubMed: 21536545]
19. Linos K, Bridge JA, Edgar MA. MUC 4-negative FUS-CREB3L2 rearranged low-grade fibromyxoid sarcoma. Histopathology. 2014;65:722–724. [PubMed: 24666374]
20. Watson S, Perrin V, Guillemot D, et al. Transcriptomic definition of molecular subgroups of small round cell sarcomas. J Pathol. 2018;245:29–40. [PubMed: 29431183]
21. Meyer C, Burmeister T, Groger D, et al. The MLL recombinome of acute leukemias in 2017. Leukemia. 2018;32:273–284. [PubMed: 28701730]
22. Lawrence HJ, Rozenfeld S, Cruz C, et al. Frequent co-expression of the HOXA9 and MEIS1 homeobox genes in human myeloid leukemias. Leukemia. 1999;13:1993–1999. [PubMed: 10602420]
23. Chen S, Dickson BC, Mohammed S, et al. A dural-based spindle cell neoplasm characterized by a novel MN1-KMT2A fusion gene. Neuro Oncol. 2019.
24. Antonescu CR, Le Loarer F, Mosquera JM, et al. Novel YAP1-TFE3 fusion defines a distinct subset of epithelioid hemangioendothelioma. Genes Chromosomes Cancer. 2013;52:775–784. [PubMed: 23737213]
25. Malgulwar PB, Nambirajan A, Pathak P, et al. C11orf95-RELA fusions and upregulated NF-KB signalling characterise a subset of aggressive supratentorial ependymomas that express L1CAM and nestin. J Neurooncol. 2018;138:29–39. [PubMed: 29354850]

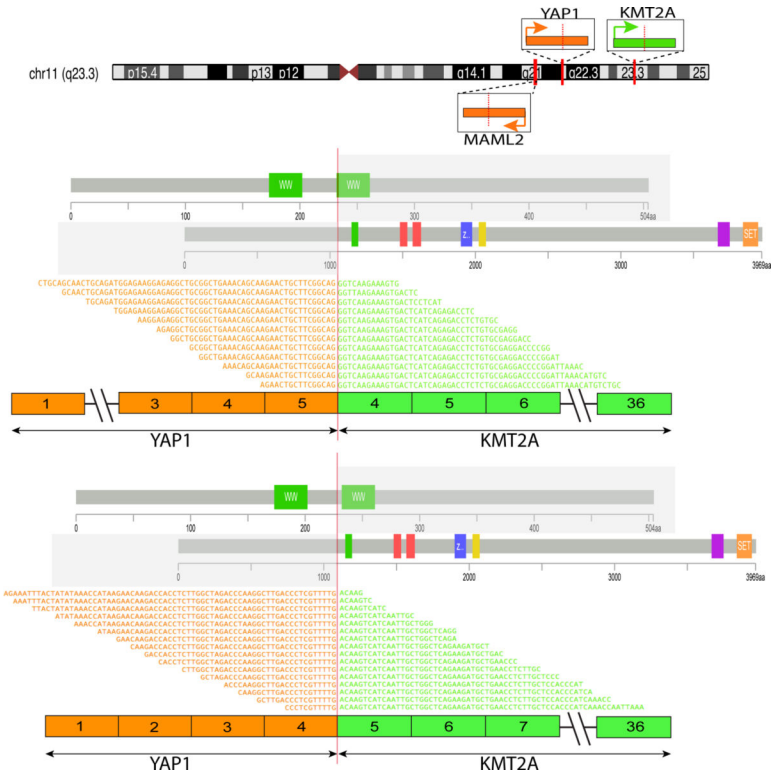

Figure 1. Diagrammatic representation of fusions involving *KMT2A, YAP1,* and *MAML2* gene.

Upper panel illustrates chromosomal locations and orientations of *KMT2A*, *YAP1*, and *MAML2* genes on chromosome 11. Middle and lower panels highlight the protein domains and exons contributed by each partner gene in the *YAP1-KMT2A* fusions, as well as the alignments of RNA sequences flanking the fusion junctions identified by RNA sequencing. *YAP1* exon 5- *KMT2A* exon 4 fusion transcripts were more common (n=3) than *YAP1* exon 4- *KMT2A* exon 5 (n=1). Both fusion variants were predicted to be in-frame.

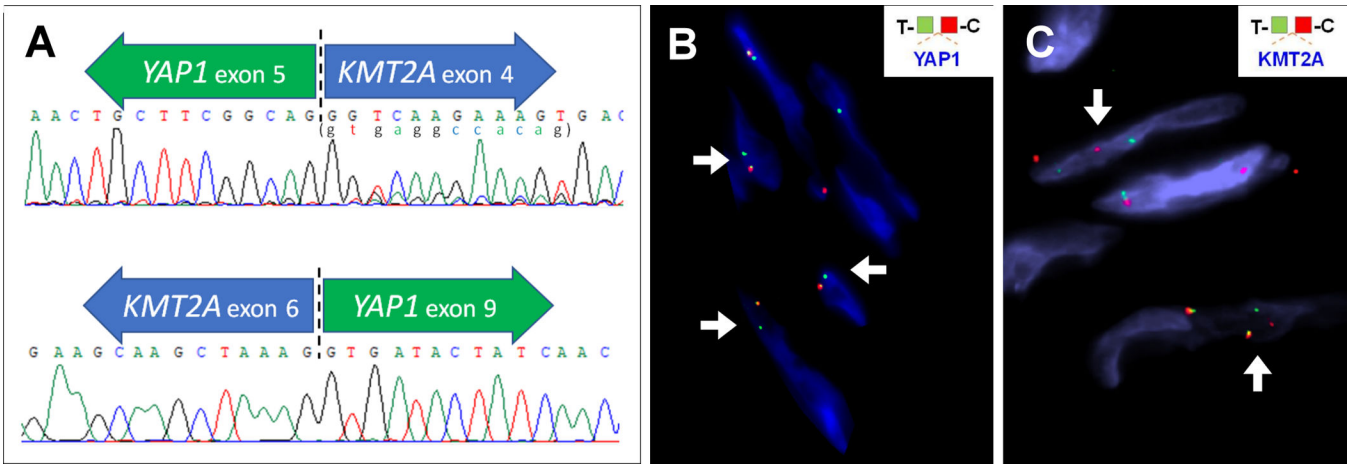

Figure 2.

(A) RT-PCR and Sanger sequencing confirmed the fusion transcripts detected by targeted RNA sequencing in case #3. A 12-bp sequence represented by minor peaks immediately starting after the breakpoint (lower case letters in parenthesis) is derived from the 5' end of *YAP1* intron 5, likely the result of alternative splicing. (B-C) FISH detected rearrangements of *YAP1* (case #3, unbalanced with 1 copy of unpaired green/telomeric signal)(B) or *KMT2A* (case #5)(C) in some cases.

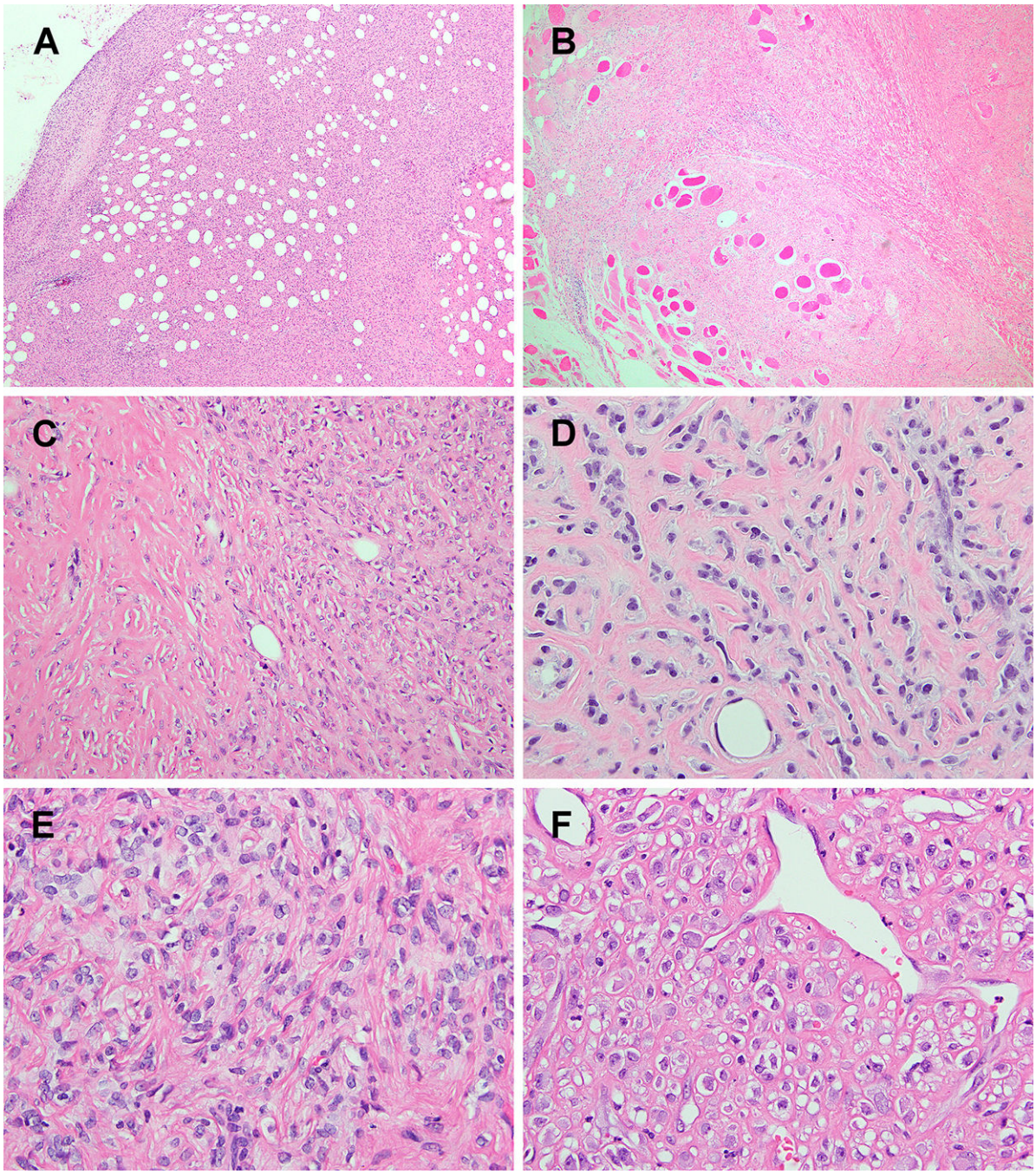

Figure 3.

The tumors often show infiltrative borders within fat (A) or skeletal muscle (B). (C) zonal variation in cellularity is a striking feature, ranging from bland-looking hypocellular regions with marked stromal sclerosis (left) to back-to-back cellularity (right). (D-F) The tumor cytology ranged from ovoid to small epithelioid cells, arranged in a cord-like pattern, frequently admixed with thick collagen fibers, morphologically consistent with SEF. The tumor cells have uniform nuclei and fine chromatin, sometimes with small distinct nucleoli. Dilated thin-walled vessels are also occasionally observed (F).

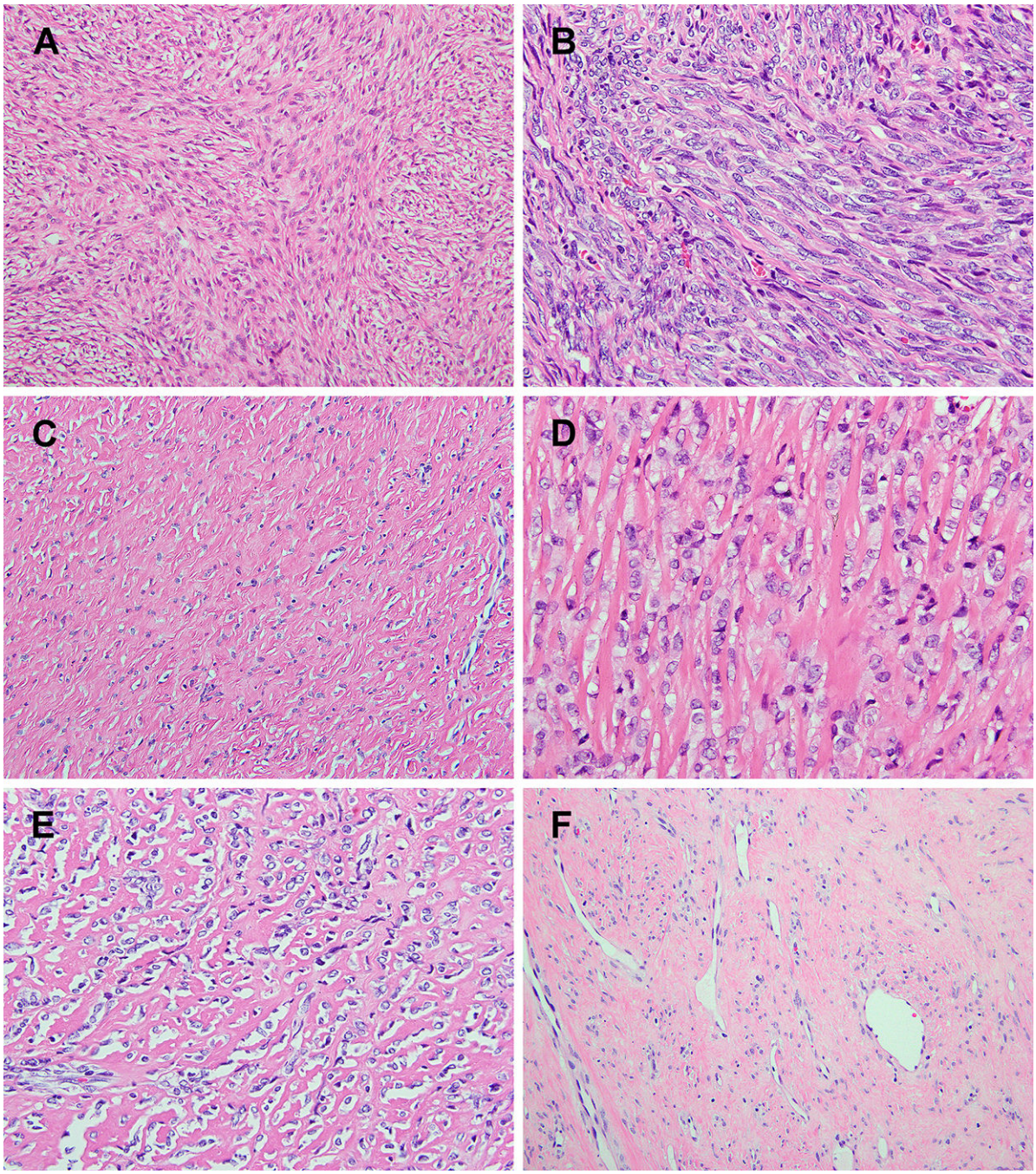

Figure 4.

Storiform and fascicular pattern of more elongated spindle cells was focally noted in some cases (A & B). All cases displayed large areas of sclerotic stroma, including a homogeneous fibrotic stroma (C), thick collagen fibers (D), and confluent collagen deposition resembling osteoid matrix (E). Deceptively hypocellular, ‘fibroma’-like areas were observed in most cases (C & F), and may lead to an erroneous diagnosis of benign lesions.

Table 1.

Sclerosing Epithelioid Fibrosarcoma with *YAP1* and/or *KMT2A* rearrangements

	Age/Sex	Location (depth)	Size (cm)	Mitotic count (10HPF)	Genetics			Follow-up
					RNAseq & RT-PCR (exon number)	*YAP1* FISH	*KMT2A* FISH	
1	45/F	Paraspinal (deep)	2.6	P: 0 R1: 1	*YAP1*(5)-*KMT2A*(4)[#]	NEG (1X)	NEG	Recur (1yr)
2	45/F	Thigh (subcutis)	3.4	P:17 Mets: 21	*YAP1*(4)-*KMT2A*(5)[#]	NEG (1X)	NEG	Mets to soft tissue (1.5yr)
3	47/M	Lower leg (deep)	2.0	P: NA R1: 5 R2: 0 R3: 2	*YAP1*(5)-*KMT2A*(4)[#†]	POS	NEG	Recur (10, 17, 21 yr)
4	73/F	Iliopsoas muscle (deep)	10	8	ND	NEG (1X)	POS	DOD (1yr), mets to contralateral pelvis & scalp
5	35/M	Chest wall (deep)	5.0	3	ND	NEG	POS[*]	Recent
6	10/F	Frontal dura (deep)	12	9	ND	NEG	POS	NED (2.5yr)
7	86/M	Inguinal (NA)	NA	11	ND	POS	NEG	NA
8	42/M	Thigh (subcutis)	2.5	4	*YAP1*(5)-*KMT2A*(4) [†]	NEG	NEG	Recent
9	22/M	Neck/paraspinal (deep)	8	4	*KMT2A(6)-YAP1(9)*[‡]	NEG (1X)	NEG (1X)	AWD (1yr)

[*] *MAML2* FISH also positive for rearrangement

[#] RNAseq

[†] RT-PCR, (parenthesis are exonic breakpoint)

[‡] MSK-IMPACT; F, female; HPF, high power fields; M, male; mets, metastasis; NA, not available; ND, not done; NEG, negative; P, primary tumor; POS, positive; R1, first recurrence; R2, second recurrence; R3, third recurrence; RNAseq, RNA sequencing; RT-PCR, reverse transcription polymerase chain reaction; yr, year(s); 1X, only one copy of fused signals.